Simulation α of EEG using brain network model

Conference Paper · December 2017

CITATIONS
0

READS
63

Auhood Jabbar
University of Southern Queensland
1 PUBLICATION **0** CITATIONS

Simulation α of EEG using brain network model

Auhood Al-Hossenat[1,2], Paul Wen[2], Yan Li[3]

[1]Faculty of Health, Engineering and Sciences,
University of Southern Queensland, Toowoomba QLD 4350, Australia
[2]University is Thi-Qar, Thi-Qar, Iraq
[3]School of Mechanical and Electrical Engineering
University of Southern Queensland, Toowoomba QLD 4350, Australia

Keywords: brain network model (BNM), neural masses model, structural connectivity, connectome, computational modelling, The Virtual Brain package

In this paper, we developed a large-scale brain network model comprising of four cerebral areas in the left hemisphere, and each area is modelled as an oscillator Jansen and Rit (JR) model. Our model is based on the structural connectivity of human connectome (SC) which was a hybrid from CoCoMac neuroinformatics database and diffusion spectrum imaging (DSI.) This brain network model was designed and implemented on the neuroinformatics platform using The Virtual Brain (TVB v1.5.3). The results demonstrated that incorporating the large-scale connectivity of brain regions and neural mass of JR model can generate signals similar to the α oscillation in frequency range of (7-12HZ) of EEG.

1. Introduction

Electroencephalography (EEG) is the recording of the brain electrical potential from the surface of the scalp using electrodes, placed on the scalp or cerebral cortex. The EEG signals is generated by the enormous synchronous dendritic activity of pyramidal cells in the cerebral cortex, which can be decomposed into distinct bands such as: delta, 1-4 Hz; theta, 4-8Hz; alpha, 7-12Hz; beta, 12-30Hz; gamma, 30-70Hz) [17]. With the availability of detailed quantitative data of anatomical connections [6, 13, 20], a new type of network models has emerged by incorporating a biologically realistic, large-scale connectivity of brain regions into dynamic network models. Recently network-modelling studies have been used to investigate the relation between structure–functional connectivity by combining the availability of full brain maps of anatomical connections with computational models of the brain's large-scale neural dynamics [2,3,4,5,7,8,12,14] .Other efforts for computational neural modelling have also been investigated the effect of altered brain anatomical connectivity on brain dynamics [1,9] which represented a unique tool for comprehension of brain diseases.

In this study, we used a large-scale brain network model including four cerebral areas in the left hemisphere. The model consists of the brain's anatomical connectivity (AC) -or connectome and neural masses of JR model. This structural connectivity given by the connectivity matrix of the human connectome is used to determine the coupling strengths among four cerebral areas in the left hemisphere. The single JR model describes the activity of each cerebral areas. The newly developed model has been generated self-sustained oscillation which reflects properties of the resting state networks observed in EEG within alpha-band between 7 and 12 HZ.

2. Materials and methods

2.1. Brain network model

The model architecture of this study based on combining both the an oscillator model which accounted the interaction of neural masses in one area and large-scale anatomical structure-or connectomes that consist of two matrices representing the strength and the time-delay of signal transmission between each pair of brain regions. The connectivity between those neural masses of a cortical patch is replaced by connections between the mean activity of populations. The general form of brain network model (BNM) equation describes the evolution of activity of a certain node in the network. This equation is computed by summing its intrinsic local dynamics (often described by a neural mass model), short -range input, long-range input from connected regions, external input could be the noise and stimuli [18].According to such strengths and time-delay matrices, the long-range input is computed by summing the scaled and delayed activity of connected nodes while the short-range input does not have a delay and the signal transmission is instantaneous. The evolution equation for brain network model used in this study is similar notation in above and paper of Spiegler and Jirsa [19], where this equation was describes by using delayed differential system. According to Spiegler and Jirsa [19] we described our model of brain network as follows: each areas in network described a neural mass of JR model , each neural mass has two state variables ,namely the mean membrane potential and mean firing rate which can describe a set $\Phi = \{\varphi_1, \varphi_2\}$. For JR model which has m=3 different neural masses (NM), namely pyramidal cells and two for excitatory and inhibitory interneuron that, the state variables of a network of m=3 NM formed as a vector $\Psi = [\Phi 1; \Phi 2 \ldots \Phi_m]$.To link state variables Ψ among 3 neural masses either excitatory or inhibitory, the square matrix of order $\sum_{i=1}^{m} ni$ is used, where n is number of variables of neural mass. By considering the interconnection I=4 of neural masses model in spatial domain, where each of them represent a single cortical areas, the state variable of the resulting brain network model formed as a vector $\Omega = [\Psi 1; \Psi 2 \ldots \Psi I]$ *according* to W_{het}, heterogeneous connectivity matrix. Thus, W_{het} can describe connectivity between 4 elements of the network (cortical areas). By applying a temporal differential operator $P\left(\frac{d}{dt}\right)$of a network of coupled Jansen and Rit local model, the temporal evolution equation of our brain network model described below with the S (Ω) is transfer function

$$P\left(\frac{d}{dt}\right)\Omega(t) = S\left(V_{loc}\Omega(t)\right) + W_{het}S\left(V_{loc}\Omega(t)\right). \quad (1)$$

2.2 Brain connectivity datasets: the connectome

This human connectome used in this study is defaulted in the neuroinformatics platform The Virtual Brain -it is publically available [2][15, 18], and is bi-hemisphere where both left and right hemispheres consist of the 38 cortical regions (listed in Table 1). Based on the default connectome in The Virtual Brain, we built the connectivity square matrix Wij, where 1≤ i ≤ n and 1≤ j≤ n, and n is the numbers of nodes in the network comprising 4 (lA1, lA2, lCCP1, lCCR2) left nodes. This matrix of connectivity defines the connection strengths and the time-delay of signal transmission between each pair of brain regions and weights the strength of the connection between the 4 brain areas by integer values from 0 to 3 with 0 representing the absence of a connection, 1 a weak connection, 2 a moderate and 3 a strong connection (see Fig 1). To quantify the connectivity characteristics and ensure the dissipation of activity in the

[2] http://thevirtualbrain.org/tvb/zwei/brainsimulator-software

network, We determined the connectivity measures for 4 nodes (lA1, lA2, lCCP, lCCR) including the in-and-out degree of connectivity-i.e. the in-out degree is the number of incoming and outgoing to /from a node, respectively.

2.3 JR neural mass model of temporal dynamics of an area

For the purpose of generating the temporal dynamics of each cortical areas, we modelled each 4 cortical areas through an isolated Jansen-Rit model and set the same standard values of the parameters on all 4 cortical areas corresponding to a JR model of a cortical column with ability to oscillate activity within the alpha-band (7-12 HZ) depend on the list of the parameter values (see Table 2; Jansen-Rit, [10]). As shown in Fig 2, the model of JR for cortical column consist of three neural masses: Pyramidal neural, local excitatory and local inhibitory neurons. Of each of them of has the state variables namely the mean membrane potentials *V(t)* and the mean firing *rates m(t)*

Label	Anatomical region	Label	Anatomical region
A1	Primary auditory cortex	PFCdm	Dorsomedial prefrontal cortex
A2	Secondary auditory cortex	PFCm	Medial prefrontal cortex
Amyg	Amygdala	PFCorb	Orbital prefrontal cortex
CCa	Anterior cingulate cortex	PFCpol	Pole of prefrontal cortex
CCp	posterior cingulate cortex	PFCvl	Ventrolateral prefrontal cortex
CCr	Retrosplenial cingulate cortex	PHC	Parahippocampal cortex
CCs	Subgenual cingulate cortex	MCdl	Dorsolateral premotor cortex
FEF	Frontal eye field	PMCm	Medial premotor cortex
G	Gustatory cortex	PMCvl	Ventrolateral premotor cortex
HC	Hippocampal cortex	S1	Primary somatosensory cortex
IA	Anterior insula	S2	Secondary somatosensory cortex
IP	Posterior insula	TCc	Central temporal cortex
M1	Primary motor area	TCi	Inferior temporal cortex
PCi	Inferior parietal cortex	TCpol	Pole of temporal cortex
PCip	Cortex of the intraparietal sulcus	TCs	superior temporal cortex
PCm	Medial parietal cortex (Precuneus)	TCv	ventral temporal cortex
PCs	Superior parietal cortex	V1	Primary visual cortex
PFCcl	Centrolateral prefrontal cortex	V2	Secondary visual cortex
PFCdl	Dorsolateral prefrontal cortex	CC	Cingulate cortex

Table 1. Anatomical labels and names of cerebral areas where the bold areas are included in our model

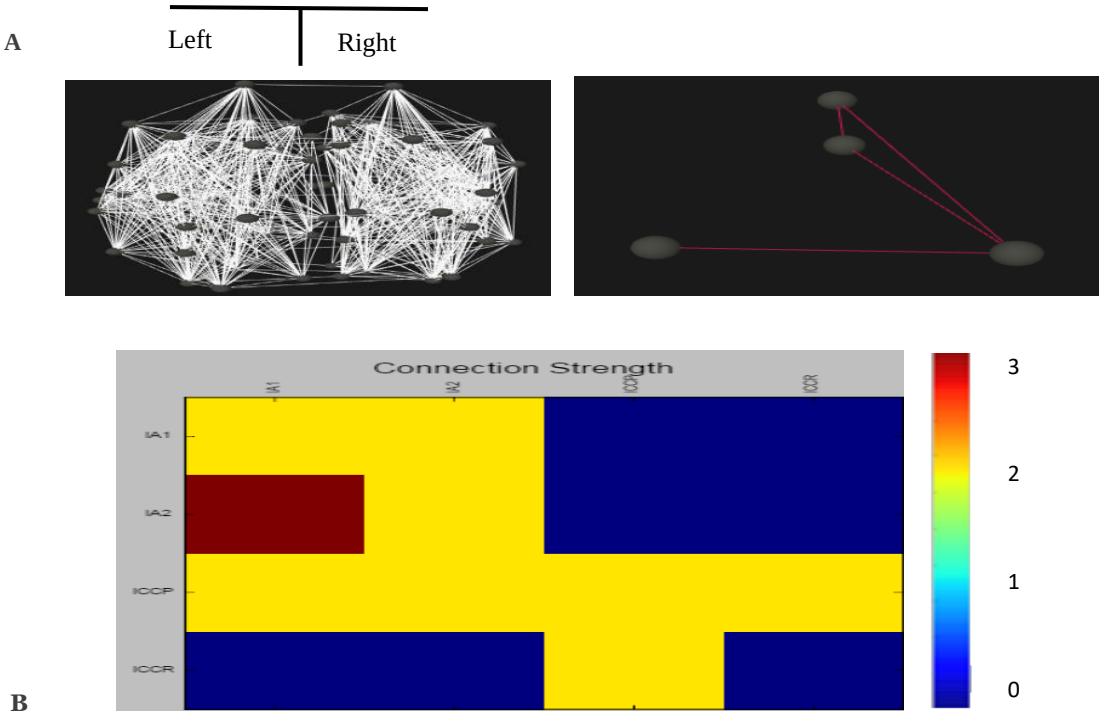

Figure 1.Structural connectivity datasets of the human for the structural layout of the brain network model .(A) left, 3-dimationonal representation of the brain network structure comprising a collection of 76 nodes(cerebral centers in black) with a collection of edges (white lines describing the long range neural fibre tracts) . Right, shows the 2-D view for network ,as projections of connectivity graph which can be represented as a connectivity matrix .(B)Connectivity matrix is arranged in columns and rows weighted to be absent, weak, moderate and strong which represented the connection strength between 4 brain regions.

Each of neurons population is modelled by two operators. The first operator converts the average pulse density of action potentials into an average postsynaptic membrane potential. This impulse response for the excitatory case and the inhibitory case is given by the functions below respectively:

$$h_e(t) = \begin{cases} Aate^{-bt} & t \geq 0 \\ 0 & else \end{cases} \quad (2)$$

$$h_i(t) = \begin{cases} Bbte^{-bt} & t \geq 0 \\ 0 & else \end{cases} \quad (3)$$

A and *B* determine the maximum amplitude of the excitatory and inhibitory postsynaptic potential (EPSP, IPSP), respectively. The second operator converts the average membrane potential of a neurons population into an average pulse density of action potentials. This transformation can be described by a nonlinear sigmoid function

$$S(V) = \frac{2eo}{1+e^{r(v0-v(t))}} \quad (4)$$

Here, e_0 determines the maximum firing rate of the neural population, v_0 is the value of potential of PSP for which 50% firing rate is achieved, r is the slope of the sigmoid at v_0; v_0 (either the firing threshold or the excitability of the populations). This model is formulated as set six first-order differential equations as follows:

$$
\begin{aligned}
\dot{y}_0(t) &= y_3(t) \\
\dot{y}_3(t) &= AaSi[y_1(t) - y_2(t)] - 2ay_3(t) - a^2 y_0(t) \\
\dot{y}_1(t) &= y_4(t) \\
\dot{y}_4(t) &= Aa\{p(t) + C_2 Si[C_1 y_0(t)]\} - 2ay_4(t) - a^2 y_1(t) \\
\dot{y}_2(t) &= y_5(t) \\
\dot{y}_5(t) &= Bb\{C_4 Si[C_3 y_0(t)]\} - 2by_5(t) - b^2 y_2(t)
\end{aligned}
\qquad (5)
$$

Thus, the temporal differential operator in below is described by a second order differential operator (see Spiegler and Jirsa ,2013 with its appendix A for more details)

$$P: D_i = \lambda^2 + 2b_i\lambda + b_i^2 \qquad (6)$$

With $b1 = b2 = 1$ and $b3 = 1 / 2$ for Pyramidal cells (i =1) with the feed loops represented by excitatory (i =2) and inhibitory (i=3).

3. Implementation and Simulation using TVB

Our model was designed and implemented by using the basis of platform TVB with its application requirements[3] including an installation guide [15]. Based on structural connectivity given by the structural connectivity matrix as shown in section of Brain connectivity datasets, we were performed the pipeline simulation (region-based) of the brain network model which brings together a neural mass model with structural data according to [15,18]. The next paragraph list the sequential steps of the simulation.

1. Bringing structural connectivity given by the connectivity matrix of the human connectome to determine the coupling strengths among 4 cerebral areas. (See section the connectome).
2. Setting long rang coupling function, it is used to join the local dynamics at distinct location over connections connectivity (i.e. it is applied to the activity propagated between regions before it enters the local dynamics equations of the model. The coupling function used in this simulation is a linear function that rescales incoming activity to a level appropriate to the population model with a slope **a** = 4.2e-8 (0.0000000042).
3. Using the conduction speed .In this study we used 4mm/ms of speed of signal propagation through the network
4. Embedding the model for the local dynamics into network. Here we used the JR'S model with its parameters. Before embedding it in a network. We identified and tuned the parameters of the local dynamics to typically used values as given in JR model (see Table 2) where this operation of parameters tune was implemented by phase plane tool in order to explore the model and how the dynamics of this physical model change as a function of its parameter. This tool is already included in TVB.
5. After we have defined our structure and dynamics of model, the numerical integration of the system was performed using Hen's method – is available for solving ordinary different equations (ODES) with an integration step size of. 0.01220703125 ms.
6. Recording the relevant data from the simulation which is simply raw neural activity described by the state variables of JR model using the Temporal average monitor with sampling period 1 ms.
7. Finally, the simulation length was 1000 ms.

[3] http://docs.thevirtualbrain.org

Model Parameter	Interpretation	Value
A	Average excitatory synaptic	3.25mV
B	Average inhibitory synaptic gain	22mV
a	Time constant of excitatory PSP	$100s^{-1}$
b	Time constant of inhibitory PSP	$50s^{-1}$
C	Average number of synaptic between populations	135
C1, C2	Average Probability of synaptic contacts in the feedback excitatory loop	C1=C C2=0.8C
C3,C4	Average Probability of synaptic contacts in the slow feedback inhibitory loop	C3=C4=0.25
v_0	The value of the average membrane potential	6Mv
V_{max}	Threshold	$5s^{-1}$
r	Steepness of the sigmoidal transformation	$0.56mV^{-1}$
e_0	The maximum firing rate of the neural population	$2.5\ s^{-1}$

Table 2. Standard Numerical Value used in Jansen's model

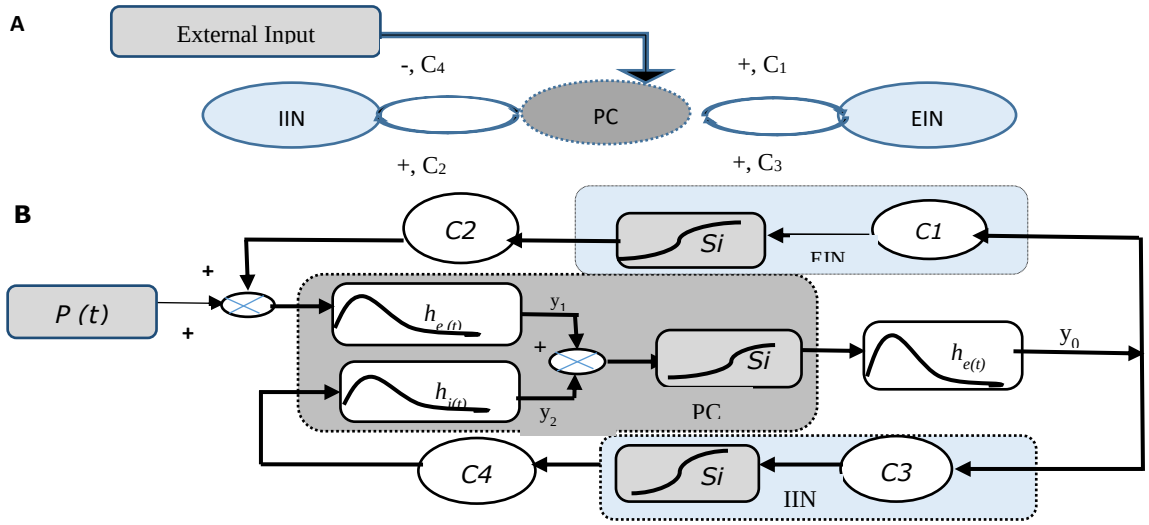

Figure 2: (A) Schematic connectivity of the Jansen & Rit model of a cortical column. Pyramidal cells *(PC)* receive excitatory and inhibitory feedback loops from local interneurons represented in populations of excitatory and inhibitory interneurons (EIN ,IIN , respectively) and excitatory input from neighboring or more distant columns ,and it give excitatory input to EIN and IIN .The arrows of excitatory and inhibitory connection marked with '+', '—', respectively. The four connectivity constants $C_{1,\dots,}$ C_4 represent the strength of the connections. (B) Block diagram of JR model which represents the mathematical operations performed inside a cortical area. The postsynaptic boxes labelled $\boldsymbol{h_{e(t)}}$ and $\boldsymbol{h_{i(t)}}$ in the figure correspond to liner synaptic integrations while the boxes labelled ***Si*** represent the cell bodies of neuros and correspond to the sigmoidal transformation hat convert the membrane potential of a neural population into an output firing rate. The constants C_i model the strength of the synaptic connections between populations and y_0, y_1 and y_2 are three main variables in the model- as the main outputs of the 3 postsynaptic boxes[10].

4. Results

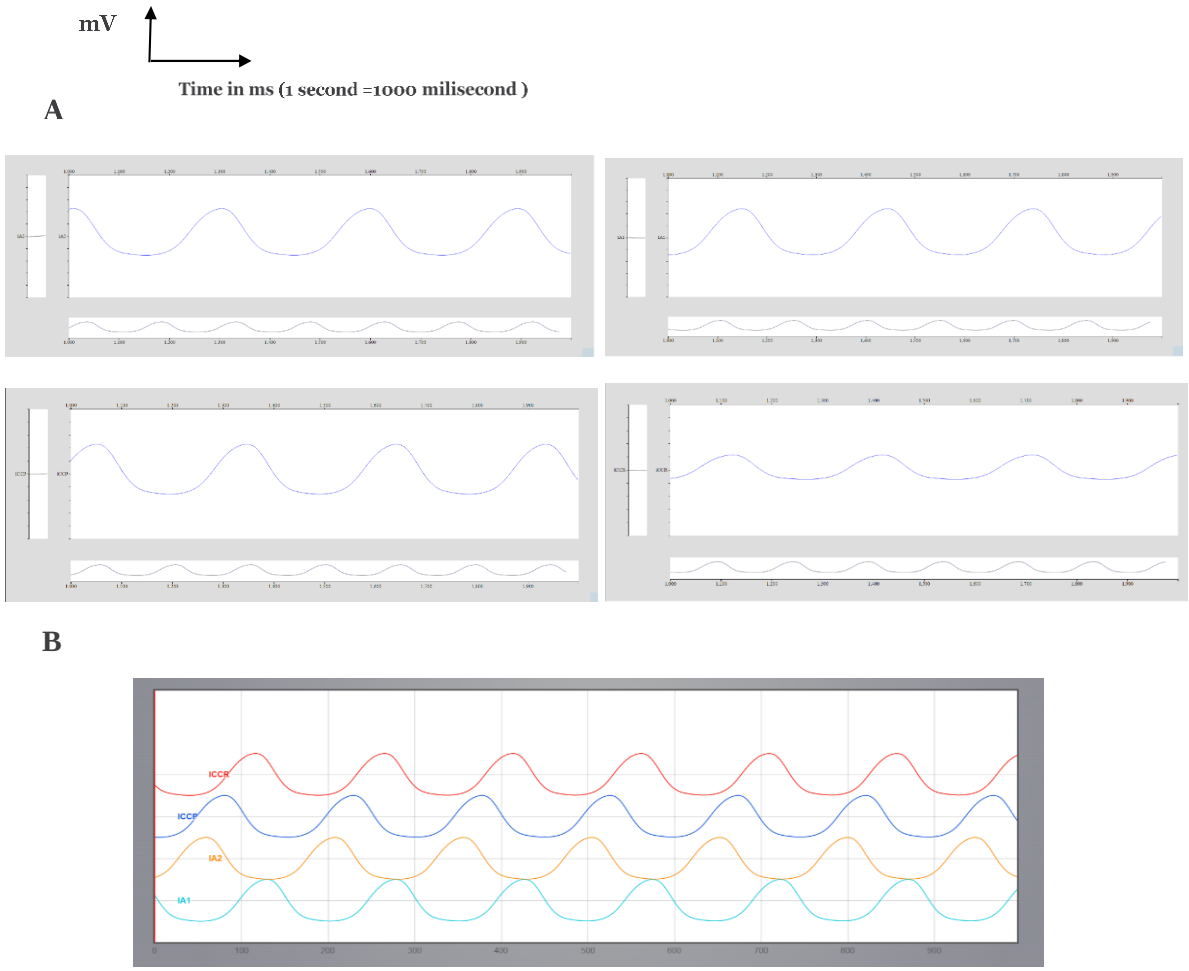

Figure 3. Simulated alpha activity. (A) Time series of each area constituted the output of the postsynaptic potential (PSP) noted $\mathbf{y_0}$ (see figure 2B) of each areas in the network in the left hemisphere. Top: lA1 and lA2. Bottom: lCCR and lCCP. (B) Time series show the simulated alpha activity for 4 left interconnected cerebral areas in the network.

Because left hemisphere appears to dominate the functions of speech, language processing and comprehension, and logical reasoning, more recently, human studies have been reported that alpha-band oscillations reflect one of the most basic cognitive processes [11] such as attention, perception, memory, language, learning, and higher reasoning and it also finds enormous interest as a potential biomarker for disorder or disease as well as playing key role in understanding other EEG phenomena due outstanding features of the alpha frequency band[16]. In this study, we have focused on this kind of oscillation generated in the left hemisphere by integrating global dynamics with a local model (mesoscopic) that determines the dynamics within brain regions. By running the Simulation steps used TVB in section above, the results of model of this study showed that the simulation of the large-scale brain network model based on Jansen-Rit population, enables to produce a signal similar to spontaneous EEG alpha oscillation within frequency range of (7-12HZ). Our finding for our large-scale brain network model depend on Jansen-Rit model represented the time series of the mean PSP of the PC noted y0,

in figure 2b of each area. This time series constituted the output of each area in the network where each area instantaneously transmitted the mean firing rate of its PC to other linked areas as shown in Figure3.

5. Discussions

We have presented a brain network model at the meso-and macroscopical scale of neural populations used here a simple neural mass –the JR model. The result from our model represented the time series of the mean postsnaptic potentials of the PC for 4 left interconnected cerebral areas in the network. We think of this quantity of y1 as the important output also as noted in figure 2b because in the cortex the PC are the main vectors of long-range cortical connections and also their electrical activity corresponds to the EEG signal. So we further simulate the mean EPSP of the PC noted y1 in figure 2b for four areas as shown in figure 4.

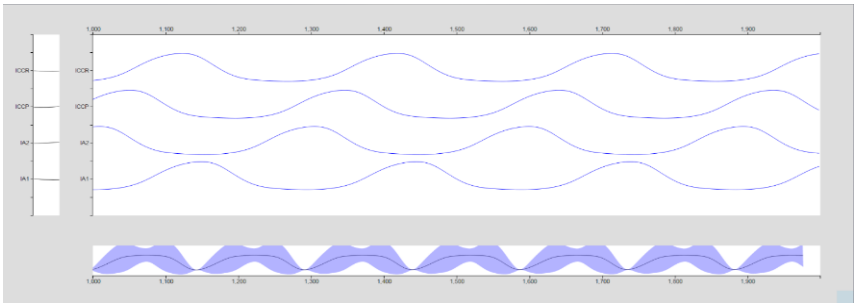

Figure 4.Time series show the simulated alpha activity for 4 left interconnected cerebral areas in the network constituted the output of the mean EPSP of the PC of each areas in the network noted y1 in figure 2b.

6. Conclusion

The focus of this study was to generate a signal similar to spontaneous EEG alpha oscillation within frequency range of (7-12Hz) using the brain network model including four cerebral areas in left hemispheres, each area is modelled by a Jansen and Rit model which accounted the interaction of neural masses in one area. The structural data used in this work is a human connectome. This model was developed and implemented on the neuroinformatics platform of The Virtual Brain (TVB v1.5.3). Our the simulation results show that the model has the potential to produce the electrical brain activity due to its performance and flexibility as well as for reproducibility of the simulations. Future studies will focus on extending the model to 38 cerebral areas in left hemisphere and also to a full model with 76 cerebral areas including both of the left and right hemispheres. The proposed model has the potential to help physicians to accurately diagnose especially with lower alpha frequency ranges for cognitive and creative tasks.

References

[1] J. Alstott, M. Breakspear, P. Hagmann, L. Cammoun, and O. Sporns, "Modeling the impact of lesions in the human brain," *PLoS Comput Biol,* vol. 5, p. e1000408, 2009.

[2] J. Cabral, E. Hugues, M. L. Kringelbach, and G. Deco, "Modeling the outcome of structural disconnection on resting-state functional connectivity," *Neuroimage,* vol. 62, pp. 1342-1353, 2012.

[3] J. Cabral, E. Hugues, O. Sporns, and G. Deco, "Role of local network oscillations in resting-state functional connectivity," *Neuroimage,* vol. 57, pp. 130-139, 2011.

[4] G. Deco, A. Ponce-Alvarez, D. Mantini, G. L. Romani, P. Hagmann, and M. Corbetta, "Resting-state functional connectivity emerges from structurally and dynamically shaped slow linear fluctuations," *Journal of Neuroscience,* vol. 33, pp. 11239-11252, 2013.

[5] A. Ghosh, Y. Rho, A. McIntosh, R. Kötter, and V. Jirsa, "Cortical network dynamics with time delays reveals functional connectivity in the resting brain," *Cognitive neurodynamics,* vol. 2, p. 115, 2008.

[6] P. Hagmann, L. Cammoun, X. Gigandet, R. Meuli, C. J. Honey, V. J. Wedeen*, et al.*, "Mapping the structural core of human cerebral cortex," *PLoS Biol,* vol. 6, p. e159, 2008.

[7] C. Honey, O. Sporns, L. Cammoun, X. Gigandet, J.-P. Thiran, R. Meuli*, et al.*, "Predicting human resting-state functional connectivity from structural connectivity," *Proceedings of the National Academy of Sciences,* vol. 106, pp. 2035-2040, 2009.

[8] C. J. Honey, R. Kötter, M. Breakspear, and O. Sporns, "Network structure of cerebral cortex shapes functional connectivity on multiple time scales," *Proceedings of the National Academy of Sciences,* vol. 104, pp. 10240-10245, 2007.

[9] C. J. Honey and O. Sporns, "Dynamical consequences of lesions in cortical networks," *Human brain mapping,* vol. 29, pp. 802-809, 2008.

[10] B. H. Jansen and V. G. Rit, "Electroencephalogram and visual evoked potential generation in a mathematical model of coupled cortical columns," *Biological cybernetics,* vol. 73, pp. 357-366, 1995.

[11] W. Klimesch, "Alpha-band oscillations, attention, and controlled access to stored information," *Trends in cognitive sciences,* vol. 16, pp. 606-617, 2012.

[12] S. Knock, A. McIntosh, O. Sporns, R. Kötter, P. Hagmann, and V. Jirsa, "The effects of physiologically plausible connectivity structure on local and global dynamics in large scale brain models," *Journal of neuroscience methods,* vol. 183, pp. 86-94, 2009.

[13] R. Kötter, "Online retrieval, processing, and visualization of primate connectivity data from the CoCoMac database," *Neuroinformatics,* vol. 2, pp. 127-144, 2004.

[14] T. Kunze, A. Hunold, J. Haueisen, V. Jirsa, and A. Spiegler, "Transcranial direct current stimulation changes resting state functional connectivity: a large-scale brain network modeling study," *Neuroimage,* vol. 140, pp. 174-187, 2016.

[15] P. S. Leon, S. A. Knock, M. M. Woodman, L. Domide, J. Mersmann, A. R. McIntosh*, et al.*, "The Virtual Brain: a simulator of primate brain network dynamics," *Frontiers in neuroinformatics,* vol. 7, 2013.

[16] N. C. Moore and M. K. Arikan, *Brainwaves and Mind: Recent Advances : a Report from Istanbul*: Kjellberg, 2004.

[17] P. L. Nunez, "The brain wave equation: a model for the EEG," *Mathematical Biosciences,* vol. 21, pp. 279-297, 1974.

[18] P. Sanz-Leon, S. A. Knock, A. Spiegler, and V. K. Jirsa, "Mathematical framework for large-scale brain network modeling in The Virtual Brain," *Neuroimage,* vol. 111, pp. 385-430, 2015.

[19] A. Spiegler and V. Jirsa, "Systematic approximations of neural fields through networks of neural masses in the virtual brain," *Neuroimage,* vol. 83, pp. 704-725, 2013.

[20] O. Sporns, "The human connectome: a complex network," *Annals of the New York Academy of Sciences,* vol. 1224, pp. 109-125, 2011.

Corresponding author's email: AuhoodHadiJabbar.Al-Hossenat@usq.edu.au